0013-7227/04/$15.00/0
Printed in U.S.A.

Endocrinology 145(7):3087–3094

doi: 10.1210/en.2003-1768

Transgenic Mice Expressing Fibroblast Growth Factor 23 under the Control of the α1(I) Collagen Promoter Exhibit Growth Retardation, Osteomalacia, and Disturbed Phosphate Homeostasis

TOBIAS LARSSON, RICHARD MARSELL, ERNESTINA SCHIPANI, CLAES OHLSSON, ÖSTEN LJUNGGREN, HARRIET S. TENENHOUSE, HARALD JÜPPNER, AND KENNETH B. JONSSON

Department of Surgical Sciences (T.L., R.M., K.B.J.), Uppsala University Hospital, SE-751 85 Uppsala, Sweden; Department of Medical Sciences (T.L., O.L.), Uppsala University Hospital, SE-751 85 Uppsala, Sweden; Endocrine Unit (E.S., H.J.), Massachusetts General Hospital and Harvard Medical School, Boston, Massachusetts 02114; Division of Endocrinology (C.O.), Department of Internal Medicine, Sahlgrenska University Hospital, SE-413 45 Gothenburg, Sweden; and Departments of Pediatrics and Human Genetics (H.S.T.), McGill University, and The McGill University-Montreal Children's Hospital Research Institute, Montreal, Quebec, Canada H3Z 2Z3

Mutations in the fibroblast growth factor 23 gene, *FGF23*, cause autosomal dominant hypophosphatemic rickets (ADHR). The gene product, FGF-23, is produced by tumors from patients with oncogenic osteomalacia (OOM), circulates at increased levels in most patients with X-linked hypophosphatemia (XLH) and is phosphaturic when injected into rats or mice, suggesting involvement in the regulation of phosphate (Pi) homeostasis. To better define the precise role of FGF-23 in maintaining Pi balance and bone mineralization, we generated transgenic mice that express wild-type human FGF-23, under the control of the α1(I) collagen promoter, in cells of the osteoblastic lineage. At 8 wk of age, transgenic mice were smaller (body weight = 17.5 ± 0.57 *vs.* 24.3 ± 0.37 g), exhibited decreased serum Pi concentrations (1.91 ± 0.27 *vs.* 2.75 ± 0.22 mmol/liter) and increased urinary Pi excretion when compared with wild-type littermates. The serum concentrations of human FGF-23 (undetectable in wild-type mice) was markedly elevated in transgenic mice (>7800 reference units/ml). Serum PTH levels were increased in transgenic mice (231 ± 62 *vs.* 139 ± 44 pg/ml), whereas differences in calcium and 1,25-dihydroxyvitamin D were not apparent. Expression of Npt2a, the major renal Na^+/Pi cotransporter, as well as Npt1 and Npt2c mRNAs, was significantly decreased in the kidneys of transgenic mice. Histology of tibiae displayed a disorganized and widened growth plate and peripheral quantitative computerized tomography analysis revealed reduced bone mineral density in transgenic mice. The data indicate that FGF-23 induces phenotypic changes in mice resembling those of patients with ADHR, OOM, and XLH and that FGF-23 is an important determinant of Pi homeostasis and bone mineralization. (*Endocrinology* 145: 3087–3094, 2004)

FIBROBLAST GROWTH FACTOR 23 (FGF-23) is a novel secreted protein encoded by a gene that is mutated in autosomal dominant hypophosphatemic rickets (ADHR) (1). Patients with ADHR exhibit clinical and biochemical characteristics that resemble those of patients with oncogenic osteomalacia (OOM) and X-linked hypophosphatemia (XLH). OOM is a paraneoplastic disease where small and usually benign tumors are associated with renal phosphate (Pi) wasting, generalized osteomalacia and muscle weakness (2). XLH is the most common form of inherited rickets and is caused by inactivating mutations in the *PHEX* gene (a Pi-regulating protein with homologies to endopeptidases encoded by a gene on the X chromosome) (3). All three disorders are characterized by hypophosphatemia due to increased renal Pi clearance, low or inappropriately normal levels of circulating 1,25-dihydroxyvitamin D_3 [1,25$(OH)_2D_3$] and rickets/osteomalacia. Current evidence indicates that FGF-23 may be involved in the pathogenesis of all three disorders.

In ADHR, missense mutations in *FGF23* (R176Q, R179W, and R179Q) change Arg residues within a subtilisin-like proprotein convertase recognition site (^{176}RHTR^{179}) (4, 5). Mammalian or insect cells expressing wild-type human FGF-23 (hFGF-23) secrete, in addition to the expected 32-kDa full-length protein, a 12- to 16-kDa carboxy-terminal fragment and a 20-kDa amino-terminal fragment (6–8). In contrast, cells expressing mutant FGF-23 secrete only the full-length protein, suggesting that the mutations prevent proteolytic processing of FGF-23 (4). There is evidence to suggest that FGF-23, or fragments thereof, may also be a substrate for PHEX, a type II membrane-associated zinc metallopeptidase that is expressed predominantly in cells of the osteoblast lineage (9–11). Although the data are conflicting, recent observations suggest that PHEX may cleave FGF-23 near the ^{176}RHTR^{179} site (12–15).

FGF-23 circulates at measurable levels in normal individuals, and serum levels are elevated in OOM patients and

Abbreviations: ADHR, Autosomal dominant hypophosphatemic rickets; BMC, bone mineral content; BMD, bone minderal density; DXA, dual x-ray absorptiometry; 1,25$(OH)_2D_3$, 1,25-dihydroxyvitamin D_3; FEI, fractional excretion index; FGF, fibroblast growth factor; H&E, hematoxylin and eosin; OOM, oncogenic osteomalacia; pDXA, peripheral DXA; PHEX, a Pi-regulating protein with homologies to endopeptidases encoded by a gene on the X chromosome; Pi, phosphate; pQCT, peripheral quantitative computerized tomography; VDR, vitamin D receptor; XLH, X-linked hypophosphatemia.

***Endocrinology* is published monthly by The Endocrine Society (http://www.endo-society.org), the foremost professional society serving the endocrine community.**

most XLH patients (16, 17). Furthermore, FGF-23 mRNA and protein are highly expressed in OOM tumors, and when these tumors are successfully removed, the circulating FGF-23 levels in patients return to within the normal range (2, 18, 19), suggesting involvement of the factor in the pathogenesis of OOM. Elevated levels of FGF-23 have also been reported in other human diseases involving disturbed Pi homeostasis, such as chronic kidney disease (20, 21) and fibrous dysplasia (22).

Direct evidence for the involvement of FGF-23 in Pi physiology came from studies where recombinant, intact FGF-23 was given parenterally to rodents or through sc implantation of cells expressing FGF-23 in immunocompromised animals. These animals develop hypophosphatemia, hyperphosphaturia, and osteomalacia (23). Data from transgenic animals expressing FGF-23 ubiquitously under the control of the CAG promoter also indicated disturbed Pi homeostasis (24), whereas ablation of the *FGF23* gene in mice resulted in significant hyperphosphatemia (25). Conflicting data on the ability of FGF-23 to inhibit Pi transport in renal cells *in vitro* (12, 26) makes it uncertain whether the effect seen in the *in vivo* models are direct or indirect. Also, it remains to be established whether the skeletal findings in these animal models are solely dependent on the systemic effects of FGF-23 or occur as result of a direct effect of FGF-23 on bone.

The tissue responsible for FGF-23 production has not been clearly identified. However, recent data demonstrate that the skeleton appears to be the major site of FGF-23 expression and that the *Hyp* mouse, which displays characteristics similar to human XLH patients, exhibits increased FGF-23 mRNA levels in calvaria, mandible, and long bones when compared with wild-type littermates (14). FGF-23 mRNA is also produced by active osteoblasts in fractures and in the lesions seen in patients with fibrous dysplasia (22).

The aim of the present study was to investigate the long-term effects of FGF-23 *in vivo*. To achieve this goal, we generated transgenic mice expressing hFGF-23 under the control of the α1(I) collagen promoter, allowing FGF-23 production in cells of the osteoblast lineage. We demonstrate in this model that FGF-23 induces phenotypic changes similar to those of patients with ADHR, OOM, and XLH and that FGF-23 is an important determinant of Pi homeostasis, vitamin D metabolism, and bone mineralization.

Materials and Methods

Generation and identification of mice expressing hFGF-23

The full-length cDNA encoding hFGF-23 was amplified by PCR from a cDNA library derived from an OOM tumor, as previously described (8). The cDNA was ligated downstream of the 2.3-kb fragment of the mouse α1(I) collagen promoter contained in the pcDNA1 vector. Restriction endonuclease digestions and nucleotide sequence analysis confirmed the correct orientation of the construct (data not shown). Nucleotide sequence analysis also confirmed the presence of an in-frame stop codon and of the native Kozak consensus sequence upstream of the translation initiation codon. The construct insert, containing the 2.3-kb fragment of the mouse α1(I) collagen promoter, 753 bp encoding hFGF-23 and 750 bp from the pcDNAI vector was released from the vector by digestion with *Hin*dIII and *Sca*I and purified according to standard techniques. Microinjections into the pronucleus of fertilized oocytes were performed at the Center for Transgene Technology (Karolinska Institute, Stockholm, Sweden). Founder mice of the F2 (CBA X C57/BL6) strain were mated with wild-type mice to establish individual transgenic lines. Mice were maintained in a virus- and parasite-free barrier facility under a 12-h light/12-h dark cycle at Uppsala University Hospital and weaned at 18 d of age onto autoclaved rodent chow containing 0.75% Pi, 0.98% calcium and 1500 U/kg vitamin D (R36, Lactamin, Stockholm, Sweden). The project was approved by the local ethics committee (approval number C 153/1).

Genotyping

For genotyping, genomic DNA was extracted from the tails using standard techniques. FGF-23 transgenic mice were detected using Southern blotting or RT-PCR with the primer pairs: forward; 5′-ctctgggtctgtgccttgtgc-3′; reverse 5′-ggagtacggggggtgggttcat-3′ (generating a fragment of 444 bp, corresponding to 123–567 of FGF-23 mRNA) or forward; 5′-ttcacttcaacaccccccatac-3′; reverse; 5′-aatagcaaagcaagcaagagt-3′ (generating a fragment of 698 bp, corresponding to 3019–3717 of the construct). For Southern blotting, the DNA was digested with *Sac*I, electrophoresed through a 1% agarose gel, blotted onto a nitrocellulose membrane (Amersham Pharmacia Biotech, Uppsala, Sweden). A full-length ^{32}P-labeled FGF-23 probe was synthesized using the Megaprime Labeling kit (Amersham Pharmacia Biotech). The membrane was hybridized at 68 C overnight (≈1 million counts/ml) in QuickHyb Hybridization Solution (Stratagene, La Jolla, CA). The membrane was rinsed in standard saline citrate buffer according to standard procedures. On autoradiographs, FGF-23 transgenic mouse DNA produced a specific band at 3.1 kb. The correct genotype was also confirmed by measuring circulating levels of hFGF-23 using an ELISA detecting the C-terminal portion of hFGF-23 (Immutopics, San Clemente, CA), which also served as assessment of expression of the transgene. Further proof of expression of the transgene was obtained by *in situ* hybridization on decalcified bone sections.

Tissue preparation

For histological analysis, mice expressing hFGF-23 and sex-matched wild-type littermates were killed by cervical dislocation at 3 d, 18 d, and 8 wk of age. Tissues from mice expressing hFGF-23 and wild-type mice were fixed in 4% formalin at 4 C overnight. In selected cases, hindlimbs were decalcified in 20% EDTA in PBS for 3 wk, and paraffin blocks were prepared by standard histological procedures. For plastic embedding, samples were fixed in 4% formalin, processed and embedded in methylmethacrylate according to standard procedure (27, 28).

Histology

Paraffin samples were cut into 6-μm sections. The sections were stained with hematoxylin and eosin (H&E). Methylmethacrylate samples were cut into 3-μm sections and stained with von Kossa and Goldner's Trichrome stain. Histology was performed on 18-d- or 8-wk-old tibiae.

In situ hybridization

A ^{35}S-labeled antisense RNA probe was transcribed from a linearized plasmid encoding hFGF-23 using a T7 RNA polymerase. The probes were purified by gel filtration through a Micro Bio-Spin chromatography column (Probe Quant, GM 50 Micro Columns, Amersham Pharmacia Biotech). Deparaffinized sections were hybridized for 12 h and then rinsed in standard saline citrate buffer according to standard procedures. The slides were covered with photographic emulsion and were exposed at 4 C for 14 d. Slides were developed and stained with H&E.

Immunohistochemistry

For immunohistochemical detection of Npt2a, frozen renal sections were fixed in 4% formalin at 4 C for 10 min. A polyclonal rabbit anti-mouse/human NPT2 (Alpha Diagnostic International, San Antonio, TX) antibody was used as primary antibody and a biotinylated IgG anti-rabbit (Vector Laboratories, Järfälla, Sweden) as secondary antibody. For development, the Avidin-Biotin-Complex kit (Vector Laboratories, Järfälla, Sweden) was used. Slides were counterstained with Mayer's hematoxylin.

Ribonuclease protection assay

Antisense RNA probes for P450c1α, P450c24 (29), Npt1, Npt2a (30), Npt2c (31), and β-actin were prepared by transcription of subcloned cDNA fragments using either T7 or T3 RNA polymerases (Maxiscript protocol, Ambion, Inc., Austin, TX) and α-^{32}P-labeled uridine triphosphate (800 Ci/mmol; NEN Life Science Products, Boston, MA). The predicted sizes of the ribonuclease-protected fragments were: P450c1α, 493 bp; P450c24, 376 bp; Npt1, 430 bp; Npt2a, 351 bp; Npt2c, 345 bp; and β-actin, 250 bp. A linearized TRIPLEscript plasmid containing a 250-bp mouse β-actin cDNA fragment was used as a control template.

The ribonuclease protection assay was performed as we described previously (31) using the HybSpeed RPA assay kit (Ambion, Inc.). Total RNA (20 μg), isolated from kidneys using the Trizol reagent (Invitrogen Life Technologies, Gaithersburg, MD), was hybridized with the appropriate riboprobes (5×10^5 cpm) at 68 C for 10 min, and treated with ribonuclease A (5 U/ml) and T1 (200 U/ml) at 37 C for 30 min. The remaining protected RNA fragments were precipitated, denatured, and resolved on a denaturing 5% acrylamide/8 M urea gel. The gel was dried and exposed to a PhosphorImager screen (Molecular Dynamics, Inc., Sunnyvale, CA) for quantitation. Results are expressed as the ratio of each transcript to β-actin mRNA.

Biochemistry

Arterial blood was collected from anesthetized animals by cutting the axillary artery. After clotting, the blood was spun and serum collected for analysis. For urine analysis, spot urine was taken four times during 24 h. Pi and calcium were measured using the phosphorous reagent kit/calcium kit (Sigma Diagnostics Inc., St. Louis, MO). Creatinine was measured at the central laboratory, Uppsala University Hospital, Sweden. All urine samples were diluted 1:10 in 0.9% NaCl. For PTH and FGF-23, the Mouse Intact PTH kit and the Human C-terminal FGF-23 ELISA kit were used (Immutopics, San Clemente, CA). 1,25(OH)$_2$D$_3$ was measured by a specific RIA kit (IDS Ltd., Boldon, UK). Urine cAMP were measured using the cAMP 200 tube kit (PerkinElmer Life Science, Boston, MA). The fractional excretion index for Pi (FEI_{π}) or calcium ($FEI_{calcium}$) was calculated as follows: FEI_{Pi} = (urine Pi/urine creatinine)/(serum Pi/serum creatinine).

Dual x-ray absorptiometry (DXA) and quantitative computerized tomography

Area bone mineral density (BMD) and bone mineral content (BMC) were measured with peripheral DXA (pDXA) Sabre and Sabre Research software (Norland Medical Systems, Inc., Fort Atkinson, WI) (32). *Ex vivo* measurements of the tibia were performed on excised bones placed on a 1-cm-thick Plexiglas table. All bones compared were measured in the same scan (high-resolution scan with line spacing set at 0.01 cm).

Computerized tomography was performed with the Stratec Peripheral QCT (pQCT) XCT Research M (software version 5.4B; Norland Medical Systems, Inc.) operating at a resolution of 70 μm (33). Middiaphyseal pQCT scans of the femur and tibia were performed to determine the cortical cross-sectional area, the cortical BMC, the periosteal circumference, and the cross-sectional moment of inertia. The middiaphyseal region of the long bones in mice contains mainly cortical bone. Metaphyseal pQCT scans of the proximal part of the tibia were performed to measure trabecular volumetric BMD. The scan was positioned in the metaphysis at a distance from the growth plate corresponding to 4.5% and 2.6% of the total length of the femur and tibia, respectively (an area containing cortical as well as trabecular bone). The trabecular bone region was defined by setting an inner threshold to 400 mg/mm^3. The interassay coefficients of variation for the pQCT measurements were less than 2%. It should be emphasized that the DXA technique gives the area BMD, whereas the pQCT gives the real/volumetric BMD. Therefore, a factor regulating the outer dimensions of a bone will affect the area BMD (DXA) but not the volumetric BMD (pQCT).

Statistical analysis

Each group studied contained 5–10 mice. Statistical analysis was performed using the Stat Soft Statistica 6 software package. Values are expressed as mean ± SEM. Differences between wild-type and transgenic groups were calculated using Student's independent *t* test. A probability of $P < 0.05$ was considered to be statistically significant.

Results

Gross phenotype of mice expressing hFGF-23

Several founder mice were identified and one viable FGF-23 transgenic line carrying the hFGF-23 transgene was established. The lines were continuously back-crossed into C57/BL6 mice, and our analysis was performed on mice in the fourth to sixth generation using wild-type littermates as controls. Incorporation of the construct was initially verified by Southern blotting using a full-length hFGF-23 probe and then with PCR as described in *Materials and Methods*. For subsequent genotyping, the C-terminal hFGF-23 ELISA (Immutopics) was used. hFGF-23 mRNA expression was confirmed with *in situ* hybridization on 3-d-old tibiae from mice expressing hFGF-23 (Fig. 1). Expression was seen in bone-forming osteoblasts, which is in agreement with the observation in other transgenic animals that have been generated using a similar promoter construct (34). The FGF-23 construct was transmitted to the progeny with the expected Mendelian frequency. The number of males and females born were similar. The gross appearance of mice expressing hFGF-23 was normal during the first week of life. However, visually detectable changes in body size, shape, and length of extremities could be observed even before the end of the weaning period. Photographic and x-ray pictures of representative 8-wk-old wild-type and FGF-23 transgenic males are displayed in Fig. 2. The mean body weight of the FGF-23 transgenic mice was significantly different at d 25, and the difference increased until adult age (Fig. 3). Mean body weights were 17.5 ± 0.57 *vs.* 24.3 ± 0.37 g for transgenic and wild-type males, respectively, ($P < 0.001$) and for females 14.8 ± 0.51 *vs.* 19.1 ± 0.67 g ($P < 0.001$). At 8 wk, tibial bone lengths were 17.8 ± 0.23 *vs.* 13.6 ± 0.21 mm for male and 17.2 ± 0.11 *vs.* 13.6 ± 0.13 mm for female wild-type and transgenic mice, respectively.

Serum and urinary biochemistry

Serum and urine parameters in male and female FGF-23 transgenic and wild-type mice were examined at 8 wk (Table

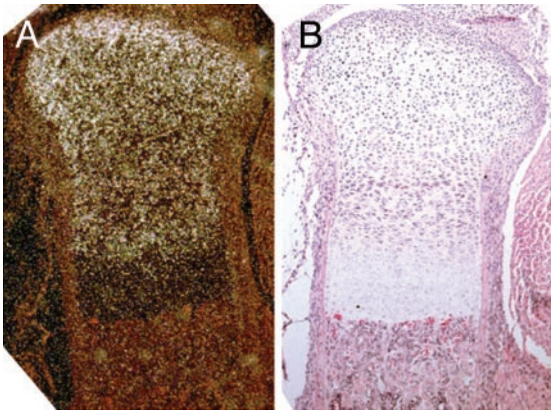

FIG. 1. Expression of transgenic construct. *In situ* hybridization with the ^{35}S-labeled full-length hFGF-23 cRNA probe on decalcified sections of tibiae from 3-d-old FGF-23 transgenic animals. High expression of hFGF-23 mRNA was seen in the epiphyseal region in osteoblastic cells. A, Dark-field; B, light-field.

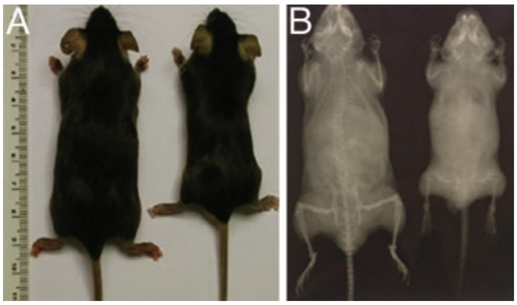

FIG. 2. Eight-week-old wild-type (*left*) and FGF-23 transgenic (*right*) mice. A, Normal photography; B, x-ray picture. Note the reduced body size as well as the general osteopenia in mice expressing hFGF-23.

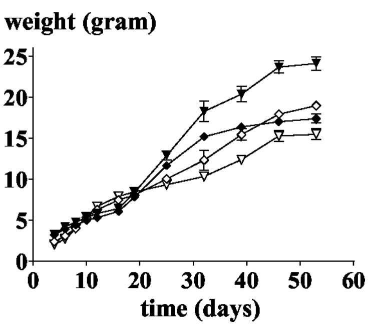

FIG. 3. Growth curves of wild-type and mice expressing hFGF-23. Measurements were performed every second day during the first 2 wk and thereafter 2 d a week until 8 wk of age. Males and females were weighed separately. ♦, Wild-type females; ▼, wild-type males; ▽, FGF-23 transgenic females; ◇, FGF-23 transgenic males. *Symbols* represent mean total body weight ± SEM for n = 6 in each group.

1A) and 18 d (Table 1B) of age. At 8 wk, mice expressing hFGF-23 revealed low serum Pi but normal serum calcium levels compared with wild-type controls. Creatinine was unchanged in FGF-23 transgenic mice compared with wild-type. Also, elevated levels of PTH were observed in FGF-23 transgenic mice. However, no difference in $1,25(OH)_2D_3$ levels were observed in mice expressing hFGF-23 compared with wild-type. Notably, female FGF-23 transgenic mice exhibited higher levels of circulating FGF-23 than male FGF-23 transgenic mice (Table 1A). Circulating PTH and $1,25(OH)_2D_3$ levels as well as Pi and calcium were also measured at d 18 (Table 1B). Already at this time point, mice expressing hFGF-23 revealed elevated PTH. In contrast to the levels in 8-wk-old mice, circulating $1,25(OH)_2D_3$ levels were significantly lower in mice expressing hFGF-23 compared with wild type.

The FEI_{Pi} and $FEI_{calcium}$ were determined. FGF-23 transgenic mice showed increased urinary Pi loss but no change in calcium excretion (Table 1A). As an increase in PTH levels was observed, urinary cAMP in 8-wk-old mice was measured. No difference in urinary cAMP levels was observed, possibly indicating a PTH resistance in mice expressing hFGF-23.

Bone phenotype

Area BMD and area BMC of 8-wk-old FGF-23 transgenic mice was determined on tibias by DXA. BMC was lower in mice expressing hFGF-23 compared with wild-type depending on decreased areal density (Table 2). To investigate the effect on different bone compartments in more detail we performed pQCT. Mice expressing hFGF-23 had decreased volumetric cortical as well as trabecular BMD in comparison to wild-type. Also, the cortical dimensions including periosteal circumference and cortical thickness were reduced. The results from these measurements are presented in Table 2.

Gross histology of bone from mice expressing hFGF-23 showed a widening of the epiphyseal growth plate, which was largely disorganized and disrupted, especially in the hypertrophic zone (Fig. 4A). Bony trabeculae in the primary spongiosa appeared to be thicker with increased connectivity but contained very little mineral (Fig. 4, A and B). Furthermore, in the secondary spongiosa, the amount of trabecular bone was reduced. Lastly, in the metaphysis, islands of chondrocytes surrounded by thick unmineralized bone matrix were observed in mice expressing hFGF-23 (Fig. 4, A and B). Von Kossa stainings generally revealed a decreased amount of mineralized matrix in FGF-23 transgenic mice (Fig. 4B). Tibiae from 18-d-old mice were examined and at this age, mineralization was also impaired (Fig. 4C). The thickness of cortical bone was reduced and both cortical and trabecular bone contained an increased amount of osteoid and decreased amounts of mineralized bone in relation to osteid (Fig. 4D).

Renal phenotype

We first examined the effect of the *hFGF23* transgene on Na^+/Pi cotransporter expression in mouse kidney. The renal abundance of the major renal Na^+/Pi cotransporter Npt2a mRNA, relative to β-actin mRNA, was significantly decreased in both male and female transgenic mice when compared with their wild-type littermates (Fig. 5A). Moreover, immunohistochemistry of renal sections revealed that Npt2a protein abundance was also reduced in mice harboring the *hFGF23* transgene (Fig. 6). Renal expression of the Npt2c (Fig. 5B) and Npt1 (males only) (Fig. 5C) mRNAs, relative to β-actin mRNA, was also significantly decreased in transgenic mice when compared with normal animals.

The expression of 1α-hydroxylase and 24α-hydroxylase mRNAs was also compared in wild-type and transgenic mice. At 8 wk, 1α-hydroxylase abundance, relative to β-actin mRNA, was reduced in transgenic male mice (not significant), but was increased in transgenic female mice (Fig. 5D). Thus, the renal 1α-hydroxylase expression followed the same pattern as the circulating levels of $1,25(OH)_2D_3$. Renal 24α-hydroxylase mRNA, relative to β-actin mRNA, was clearly increased in transgenic males and also in females (not significant) (Fig. 5E).

Parathyroid glands

To further explore the elevated levels of circulating PTH in mice expressing hFGF-23, we examined the parathyroid glands histologically at 8 wk. The parathyroid glands in mice expressing hFGF-23 were hypertrophic, but no structural changes were observed (Fig. 7).

TABLE 1. Serum and urinary biochemistry

	Male (wild-type)	Male (FGF-23 transgenic)	Female (wild-type)	Female (FGF-23 transgenic)
A				
Pi (mM)	2.75 ± 0.22	1.91 ± 0.27[a]	2.16 ± 0.15	1.19 ± 0.11[a]
Calcium (mM)	2.17 ± 0.10	2.07 ± 0.09	2.12 ± 0.05	2.08 ± 0.05
Creatinine (μM)	56 ± 5.8	55 ± 2.3	55 ± 2.2	49 ± 2.9
PTH (pg/ml)	139 ± 44	231 ± 62[b]	167 ± 38	321 ± 47[b]
1,25(OH)$_2$D$_3$ (pg/ml)	261 ± 22	254 ± 12	143 ± 28	172 ± 25
FGF-23 (RU/ml)	Not detectable	7,800 ± 800	Not detectable	17,600 ± 3,500
FEI(Pi)	14.5 ± 2.5	34.8 ± 7.6[a]	14.0 ± 3.8	72.3 ± 31[b]
FEI(calcium)	19.7 ± 7.7	17.1 ± 4.6	11.9 ± 2.8	18.2 ± 3.0
cAMP (pmol/ml)	36,400 ± 6,500	40,400 ± 14,200	31,800 ± 2,900	37,400 ± 5,900
B				
Pi (mM)	3.17 ± 0.16	1.76 ± 0.10[a]	3.20 ± 0.12	2.24 ± 0.15[a]
Calcium (mM)	2.31 ± 0.05	2.18 ± 0.03	2.30 ± 0.06	2.33 ± 0.07
PTH (pg/ml)	77 ± 15	242 ± 30[a]	31 ± 10	155 ± 20[a]
1,25(OH)$_2$D$_3$ (pg/ml)	658 ± 122	292 ± 66[b]	761 ± 294	274 ± 84

Serum samples were collected at 8 wk (A) and 18 d (B). Urinary samples were collected at 8 wk. Differences between FGF-23 wild-type and transgenic mice were calculated for males and females separately. Significance levels are: [a] $P < 0.001$; [b] $P < 0.05$.

TABLE 2. Results from DXA and pQCT measurements of tibiae in FGF-23 transgenic and wild-type mice

	Male (wild-type)	Male (FGF-23 transgenic)	Female (wild-type)	Female (FGF-23 transgenic)
BMD (cm^2)	0.045 ± 0.003	0.026 ± 0.0008[a]	0.046 ± 0.0006	0.030 ± 0.0009[a]
BMC (g)	0.021 ± 0.002	0.008 ± 0.0006[a]	0.018 ± 0.0006	0.008 ± 0.0005[a]
Area (cm^2)	0.46 ± 0.02	0.31 ± 0.01[a]	0.39 ± 0.009	0.265 ± 0.011[a]
Trabecular density (mg/cm^3)	297 ± 32	69 ± 7.8[a]	274 ± 10.5	140 ± 10.9[a]
Cortical density (mg/cm^3)	898 ± 8.9	631 ± 17.3[a]	886 ± 7.1	666 ± 14.1[a]
Cortical thickness (mm)	0.37 ± 0.11	0.24 ± 0.008[a]	0.35 ± 0.003	0.23 ± 0.004[a]
Periosteal circumference (mm)	4.87 ± 0.14	3.76 ± 0.09[a]	4.55 ± 0.05	3.63 ± 0.05[a]

Differences between FGF-23 transgenic and wild-type mice were calculated for males and females separately. All variables were different at a significance level of $P < 0.001$ ([a]).

Discussion

The principal finding of this study is that mice expressing FGF-23 in bone tissue develop a severe skeletal phenotype characterized by osteomalacia and disturbed growth plate architecture. In addition, the FGF-23 transgenic mice are hypophosphatemic secondary to increased renal Pi clearance resulting from decreased renal expression of the Na^+/Pi cotransporter genes, Npt2a, Npt2c, and Npt1. Finally, the transgenic mice show paradoxically low/normal 1,25(OH)$_2$D$_3$ levels. Our data thus indicate that FGF-23 is an important regulator of Pi homeostasis and vitamin D metabolism. This conclusion is supported by several previous studies of systemic FGF-23 overexpression (5, 23, 24) and by a study describing the targeted deletion of the *FGF23* gene (25).

Recent reports suggest that FGF-23 is expressed mainly in active osteoblastic cells (15). FGF-23 expression is also seen in the histologically disorganized bone lesions of fibrous dysplasia (22). It is unclear whether bone derived FGF-23 is acting locally on bone cells or whether its actions are endocrine. In our model, FGF-23 is produced in bone. However, FGF-23 is readily secreted and released into the circulation and high levels of circulating FGF-23 were observed in this transgenic model. Our data, therefore, cannot differentiate between local skeletal actions and systemic effects of FGF-23.

The skeletal phenotype of the FGF-23 transgenic mice share many characteristics with other rachitic animal models. For example the Hyp mouse, which carries a deletion of the *PHEX* gene, shows a similar bone phenotype as well as hypophosphatemia secondary to decreased renal expression of Npt2a, Npt2c, and Npt1 (31). Notably, circulating levels of FGF-23 are elevated approximately 20-fold in this model (35) (Tenenhouse, H. S., and T. Yamashita, unpublished data). It is possible that the bone phenotype in the Hyp and the FGF-23 transgenic models could be caused by insufficient Pi at the mineralization front. However, Npt2a knockout mice do not exhibit rickets and osteomalacia despite significant hypophosphatemia (36, 37). Moreover, in that model, PHEX expression is intact (31) and serum levels of FGF-23 are significantly lower relative to wild-type littermates (Tenenhouse, H. S., and T. Yamashita, unpublished data). This suggests that mechanisms other than hypophosphatemia are involved in the development of rickets in the animal model presented here.

It is well known that lack of vitamin D, as in the 1α(OH)ase null mice (38), or lack of vitamin D receptor (VDR) signaling, as in the VDR knockout, causes rickets and osteomalacia. Because vitamin D metabolism in FGF-23 transgenic animals is disturbed, this could contribute to the rickets observed. In the VDR null mice, the hypertrophic chondrocyte layer exhibits decreased apoptosis (39) and *in vitro* data suggest that Pi is capable of inducing apoptosis in chondrocytes (40). However, a histologically normal growth plate can be maintained in the VDR null mice (41) by increasing the intake of dietary calcium and phosphorous. Thus, neither hypophosphatemia alone nor vitamin D deficiency, under conditions where the supply of calcium and phosphorous is adequate, is sufficient to induce rickets/osteomalacia. We therefore propose that other effects of FGF-23 contribute to demineralization of bone.

Hypophosphatemia is normally a strong stimulator of the

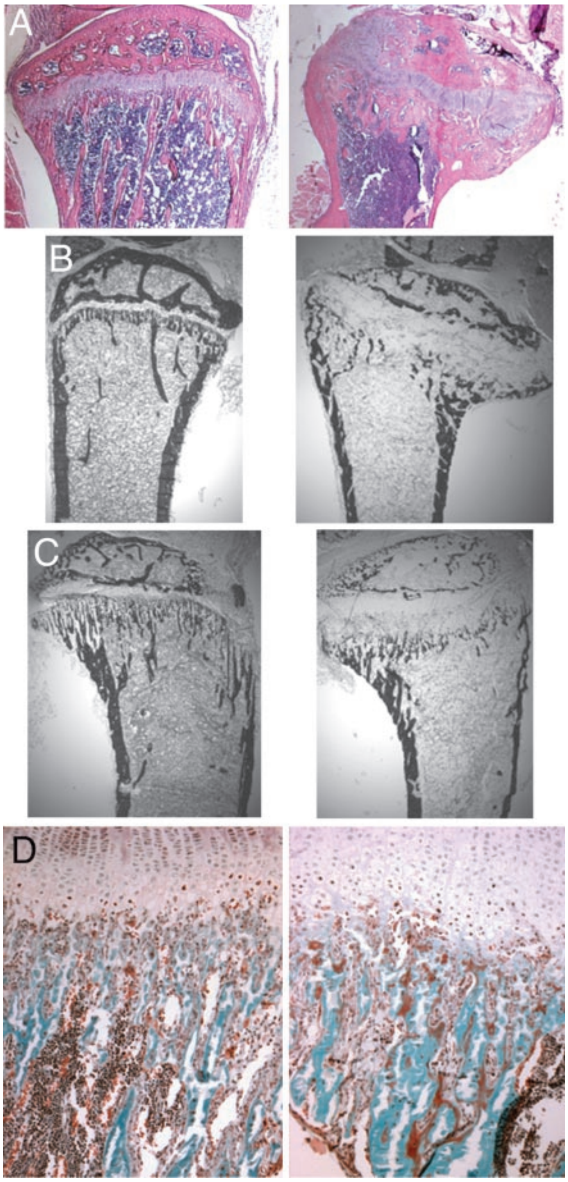

FIG. 4. Bone histology. A, H&E staining of 8-wk-old mice showed a widened and disrupted growth plate in mice expressing hFGF-23 (*right*) compared with wild-type (*left*). B, Von Kossa staining of tibial sections from 8-wk-old mice indicated a reduced amount of mineralized bone (*black*) in mice expressing hFGF-23 (*bottom*) compared with wild-type (*top*). C, Von Kossa staining of tibial sections from 18-d-old mice indicated reduced mineralization at this age. FGF-23 transgenic (*bottom*) and wild-type (*top*) mice. D, Trichrome staining of tibial sections from 8-wk-old mice showed increased amounts of osteoid (*red*) around the growth plate in mice expressing hFGF-23 (*right*) compared with wild-type (*left*). Also, decreased amounts of mineralized bone (*green*) in relation to osteid were observed in mice expressing hFGF-23.

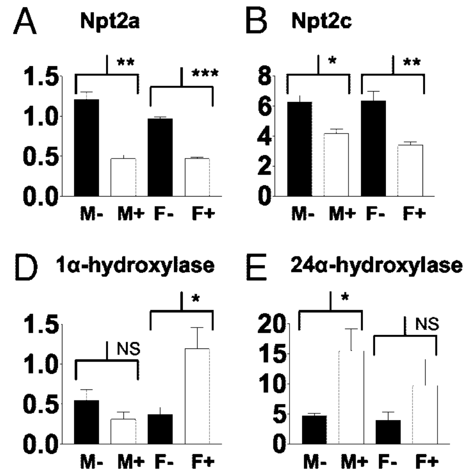

FIG. 5. Ribonuclease protection assay: relative levels of mRNA encoding renal Pi transporters Npt2a (A); Npt2c (B); and Npt1 (C) revealed a down-regulation of all three transporters. Renal expression of 1α-hydroxylase mRNA was reduced in male transgenic mice (not significant) but increased in female transgenic mice (D), whereas there was an increase of 24-hydroxylase mRNA expression (E). Wild-type mice in *filled bars* and FGF-23 transgenic mice in *open bars*. Significance levels (indicated in *brackets*) are *, $P < 0.05$; **, $P < 0.01$; and ***, $P < 0.001$.

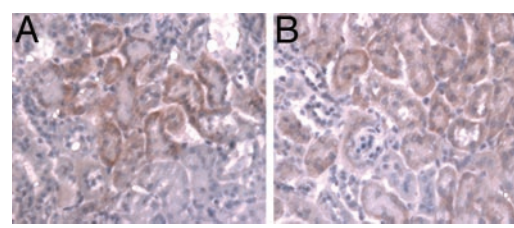

FIG. 6. Immunohistochemistry on frozen renal sections showed decreased amounts of Npt2a protein in mice expressing hFGF-23 (B) compared with wild-type (A).

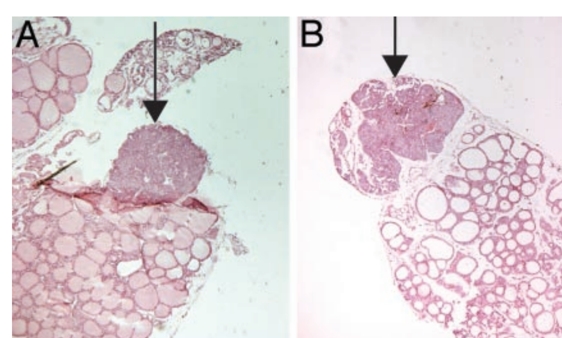

FIG. 7. Histology of the parathyroid glands (indicated by *arrows*) showing hypertrophic glands in FGF-23 transgenic (B) compared with wild-type mice (A), indicating development of secondary hyperparathyroidism.

renal 1α-hydroxylase, leading to a rise in the serum concentration of $1,25(OH)_2D_3$ (42). However, in young FGF-23 transgenic mice, $1,25(OH)_2D_3$ levels are inappropriately low. This suggests dysregulation of vitamin D metabolism in the presence of high circulating levels of FGF-23. Indeed, this is a hallmark of hypophosphatemic disorders in which high levels of FGF-23 have been demonstrated. For example, patients with OOM and XLH have either low or normal serum $1,25(OH)_2D_3$ levels in the face of significant hypophosphatemia (16, 17). Also, in contrast to the Npt2a knockout mice, which have elevated serum $1,25(OH)_2D_3$ levels (29), Hyp mice have inappropriately normal $1,25(OH)_2D_3$ levels and also fail to respond to a low Pi challenge with increased renal 1α-hydroxylase activity and elevated serum $1,25(OH)_2D_3$

(29, 43). This suggests that FGF-23 modulates the increased activity of the 1α-hydroxylase in response to low Pi intake. Furthermore, as in the case of Hyp mice, FGF-23 transgenic mice clearly have increased expression of 24-hydroxylase mRNA in their kidneys (43). The latter could contribute to the inability of Hyp mice and FGF-23 transgenic mice to increase their serum $1,25(OH)_2D_3$ concentration in response to hypophosphatemia.

In adult mice, the difference between circulating $1,25(OH)_2D_3$ levels in wild-type compared with FGF-23 transgenic animals disappeared. This could be due to an adaptive mechanism in the renal cells expressing 1α-hydroxylase or the result of a FGF-23 receptor down-regulation. More likely, the development of secondary hyperparathyroidism may facilitate the maintenance of normal levels of $1,25(OH)_2D_3$ because PTH is a known stimulator of 1α-hydroxylase mRNA and $1,25(OH)_2D_3$ production (44). Interestingly, 1α-hydroxylase mRNA levels were higher in female than in male transgenic mice. The reason for this remains unclear but could be related to differences in the levels of systemic Phex expression or to sex-specific hormonal differences. Of note, FGF-23 levels were for unknown reasons also higher in female than in male transgenic mice.

PTH levels were clearly raised in FGF-23 transgenic mice as early as 18 d of age and remained increased in adulthood. Histology of the parathyroid glands demonstrates hypertrophy but no adenomas. The elevated levels of PTH in the FGF-23 transgenic animals, as well as in Hyp mice (45, 46) may be crucial for maintaining normocalcemia because Hyp mice with targeted deletion of the PTH gene suffer from early lethality due to hypocalcemia (47). The elevated PTH levels in the Hyp and FGF-23 transgenic mouse models may also contribute to the renal Pi wasting and ensuing hypophosphatemia (45, 46).

The cause of the secondary hyperparathyroidism in the FGF-23 transgenic animals is not entirely clear. The mice expressing hFGF-23 had normal serum calcium levels, and no increase in urinary calcium excretion. Additionally, low Pi levels should counteract development of parathyroid gland hypertrophy because Pi *per se* is known to stimulate parathyroid cell proliferation (48). It is possible that the inappropriately low levels of $1,25(OH)_2D_3$ may contribute to the parathyroid hypertrophy. $1,25(OH)_2D_3$ has a direct suppressive effect on the parathyroid gland (49, 50) and lack of $1,25(OH)_2D_3$ could therefore potentially lead to the observed hypertrophy. It remains to be investigated whether FGF-23 has a direct stimulatory effect on the chief cells in the parathyroid glands. Interestingly, patients with renal failure have been found to have high levels of circulating FGF-23 in the setting of low $1,25(OH)_2D_3$ and secondary hyperparathyroidism (20, 21). Thus, the FGF-23 transgenic mouse model offers new opportunities to study the relative contribution of low $1,25(OH)_2D_3$, low Pi, and high FGF-23 to the development of secondary hyperparathyroidism.

Normal serum Pi levels are maintained mainly through the regulation of Npt2a activity in the kidneys (36). Although a specific Pi sensor has not yet been identified, it is well established that the kidney responds to changes in dietary Pi intake (51) by adjusting the reabsorption of filtered Pi from the proximal tubule. Pi deprivation leads to up-regulation of Npt2a, whereas Pi loading down-regulates Npt2a and thus increases urinary excretion of Pi (52). Npt2a is also a target for the regulation of renal Pi reabsorption by PTH (52, 53). We found that renal Npt2a mRNA and protein expression are clearly decreased in FGF-23 transgenic mice, explaining the mechanism for the urinary loss of Pi and subsequent hypophosphatemia. The down-regulation of Npt2a despite the long-term hypophosphatemia prevailing in the FGF-23 transgenic mice indicates that FGF-23 may act directly to reduce renal Npt2a expression. Notably, it was recently reported that FGF-23 down-regulates Npt2a expression in opossum kidney cells through FGFR3 signaling (26). We also found reduced renal mRNA expression of other sodium-dependent Pi transporters, including the less abundantly expressed Npt1 (54), and the novel renal brush-border membrane cotransporter Npt2c (31). Taken together, our data suggest that the FGF-23-mediated decrease in renal Pi reabsorption in the transgenic model may be the result of the down-regulation of all three sodium/Pi cotransporters, consistent with similar findings recently reported in Hyp mice (31).

In summary, this study describes a novel transgenic mouse model in which FGF-23 is overexpressed in cells of the osteoblast lineage. These transgenic animals are likely to provide further insights into the physiological role of FGF-23 in Pi homeostasis and bone biology.

Acknowledgments

We thank Anna-Lena Johansson for technical assistance; Karolinska Center for Transgene Technologies (Stockholm, Sweden) for construct injections; and Per Hellman (Department of Surgical Sciences, Uppsala University Hospital, Uppsala, Sweden) for surgical removal of the parathyroid glands.

Received December 31, 2003. Accepted February 18, 2004.

Address all correspondence and requests for reprints to: Kenneth B. Jonsson, Department of Surgical Sciences, University Hospital, SE-751 85, Uppsala, Sweden. E-mail: Kenneth.Jonsson@surgsci.uu.se.

This work was supported by grants from the Swedish Research Council, Genzyme Renal Innovation Programe, the Swedish Society of Medicine and Canadian Institutes of Health Research [FRN 44345 (to H.S.T.)].

T.L. and R.M. contributed equally to this work.

References

1. 2000 Autosomal dominant hypophosphataemic rickets is associated with mutations in FGF-23. The ADHR Consortium. Nat Genet 26:345–348
2. **Cotton GE** 1994 Oncogenic osteomalacia. N Engl J Med 331:1023
3. 1995 A gene (PEX) with homologies to endopeptidases is mutated in patients with X-linked hypophosphatemic rickets. The HYP Consortium. Nat Genet 11:130–136
4. **White KE, Carn G, Lorenz-Depiereux B, Benet-Pages A, Strom TM, Econs MJ** 2001 Autosomal-dominant hypophosphatemic rickets (ADHR) mutations stabilize FGF-23. Kidney Int 60:2079–2086
5. **Bai XY, Miao D, Goltzman D, Karaplis AC** 2003 The autosomal dominant hypophosphatemic rickets R176Q mutation in fibroblast growth factor 23 resists proteolytic cleavage and enhances in vivo biological potency. J Biol Chem 278:9843–9849
6. **White KE, Jonsson KB, Carn G, Hampson G, Spector TD, Mannstadt M, Lorenz-Depiereux B, Miyauchi A, Yang IM, Ljunggren O, Meitinger T, Strom TM, Jüppner H, Econs MJ** 2001 The autosomal dominant hypophosphatemic rickets (ADHR) gene is a secreted polypeptide overexpressed by tumors that cause phosphate wasting. J Clin Endocrinol Metab 86:497–500
7. **Shimada T, Muto T, Urakawa I, Yoneya T, Yamazaki Y, Okawa K, Takeuchi Y, Fujita T, Fukumoto S, Yamashita T** 2002 Mutant FGF-23 responsible for autosomal dominant hypophosphatemic rickets is resistant to proteolytic cleavage and causes hypophosphatemia *in vivo*. Endocrinology 143:3179–3182
8. **Larsson T, Zahradnik R, Lavigne J, Ljunggren O, Jüppner H, Jonsson KB** 2003 Immunohistochemical detection of FGF-23 protein in tumors that cause oncogenic osteomalacia. Eur J Endocrinol 148:269–276

9. **Thompson DL, Sabbagh Y, Tenenhouse HS, Roche PC, Drezner MK, Salisbury JL, Grande JP, Poeschla EM, Kumar R** 2002 Ontogeny of Phex/PHEX protein expression in mouse embryo and subcellular localization in osteoblasts. J Bone Miner Res 17:311–320
10. **Ruchon AF, Tenenhouse HS, Marcinkiewicz M, Siegfried G, Aubin JE, DesGroseillers L, Crine P, Boileau G** 2000 Developmental expression and tissue distribution of Phex protein: effect of the Hyp mutation and relationship to bone markers. J Bone Miner Res 15:1440–1450
11. **Ecarot B, Desbarats M** 1999 1,25-$(OH)_2D_3$ Down-regulates expression of Phex, a marker of the mature osteoblast. Endocrinology 140:1192–1199
12. **Bowe AE, Finnegan R, Jan de Beur SM, Cho J, Levine MA, Kumar R, Schiavi SC** 2001 FGF-23 inhibits renal tubular phosphate transport and is a PHEX substrate. Biochem Biophys Res Commun 284:977–981
13. **Campos M, Couture C, Hirata IY, Juliano MA, Loisel TP, Crine P, Juliano L, Boileau G, Carmona AK** 2003 Human recombinant PHEX has a strict S1′ specificity for acidic residues and cleaves peptides derived from FGF-23 and MEPE. Biochem J 373(Pt 1):271–279
14. **Liu S, Guo R, Simpson LG, Xiao ZS, Burnham CE, Quarles LD** 2003 Regulation of fibroblastic growth factor 23 expression but not degradation by PHEX. J Biol Chem 278:37419–37426
15. **Quarles LD** 2003 FGF-23, PHEX, and MEPE regulation of phosphate homeostasis and skeletal mineralization. Am J Physiol Endocrinol Metab 285: E1–E9
16. **Yamazaki Y, Okazaki R, Shibata M, Hasegawa Y, Satoh K, Tajima T, Takeuchi Y, Fujita T, Nakahara K, Yamashita T, Fukumoto S** 2002 Increased circulatory level of biologically active full-length FGF-23 in patients with hypophosphatemic rickets/osteomalacia. J Clin Endocrinol Metab 87:4957–4960
17. **Jonsson KB, Zahradnik R, Larsson T, White KE, Sugimoto T, Imanishi Y, Yamamoto T, Hampson G, Koshiyama H, Ljunggren O, Oba K, Yang IM, Miyauchi A, Econs MJ, Lavigne J, Jüppner H** 2003 Fibroblast growth factor 23 in oncogenic osteomalacia and X-linked hypophosphatemia. N Engl J Med 348:1656–1663
18. **Nelson AE, Mason RS, Robinson BG, Hogan JJ, Martin EA, Ahlstrom H, Astrom G, Larsson T, Jonsson K, Wibell L, Ljunggren O** 2001 Diagnosis of a patient with oncogenic osteomalacia using a phosphate uptake bioassay of serum and magnetic resonance imaging. Eur J Endocrinol 145:469–476
19. **White KE, Waguespack SG, Econs MJ** 2002 Case 29–2001: oncogenic hypophosphatemic osteomalacia. N Engl J Med 346:381–382
20. **Weber TJ, Liu S, Indridason OS, Quarles LD** 2003 Serum FGF-23 levels in normal and disordered phosphorus homeostasis. J Bone Miner Res 18:1227–1234
21. **Larsson T, Nisbeth U, Ljunggren O, Jüppner H, Jonsson KB** 2003 Circulating concentration of FGF-23 increases as renal function declines in patients with chronic kidney disease, but does not change in response to variation in phosphate intake in healthy volunteers. Kidney Int 64:2272–2279
22. **Riminucci M, Collins MT, Fedarko NS, Cherman N, Corsi A, White KE, Waguespack S, Gupta A, Hannon T, Econs MJ, Bianco P, Gehron Robey P** 2003 FGF-23 in fibrous dysplasia of bone and its relationship to renal phosphate wasting. J Clin Invest 112:683–692
23. **Shimada T, Mizutani S, Muto T, Yoneya T, Hino R, Takeda S, Takeuchi Y, Fujita T, Fukumoto S, Yamashita T** 2001 Cloning and characterization of FGF-23 as a causative factor of tumor-induced osteomalacia. Proc Natl Acad Sci USA 98:6500–6505
24. **Shimada T, Urakawa I, Yamazaki Y, Hasegawa H, Hino R, Yoneya T, Takeuchi Y, Fujita T, Fukumoto S, Yamashita T** 2004 FGF-23 transgenic mice demonstrate hypophosphatemic rickets with reduced expression of sodium phosphate cotransporter type IIa. Biochem Biophys Res Commun 314:409–414
25. **Shimada T, Kakitani M, Yamazaki Y, Hasegawa H, Takeuchi Y, Fujita T, Fukumoto S, Tomizuka K, Yamashita T** 2004 Targeted ablation of Fgf23 demonstrates an essential physiological role of FGF23 in phosphate and vitamin D metabolism. J Clin Invest 113:561–568
26. **Yamashita T, Konishi M, Miyake A, Inui K, Itoh N** 2002 Fibroblast growth factor (FGF)-23 inhibits renal phosphate reabsorption by activation of the mitogen-activated protein kinase pathway. J Biol Chem 277:28265–28270
27. **Erben RG** 1997 Embedding of bone samples in methylmethacrylate: an improved method suitable for bone histomorphometry, histochemistry, and immunohistochemistry. J Histochem Cytochem 45:307–313
28. **Schenk R OA, Herrmann W** 1984 Preparation of calcified tissues for light microscopy. In: Dickson G, ed. Methods of calcified tissue preparation. Amsterdam: Elsevier; 56
29. **Tenenhouse HS, Martel J, Gauthier C, Zhang MY, Portale AA** 2001 Renal expression of the sodium/phosphate cotransporter gene, Npt2, is not required for regulation of renal 1 α-hydroxylase by phosphate. Endocrinology 142: 1124–1129
30. **Tenenhouse HS, Roy S, Martel J, Gauthier C** 1998 Differential expression, abundance, and regulation of Na+-phosphate cotransporter genes in murine kidney. Am J Physiol 275:F527–F534
31. **Tenenhouse HS, Martel J, Gauthier C, Segawa H, Miyamoto K** 2003 Differential effects of Npt2a gene ablation and X-linked Hyp mutation on renal expression of Npt2c. Am J Physiol Renal Physiol 285:F1271–F1278
32. **Windahl SH, Vidal O, Andersson G, Gustafsson JA, Ohlsson C** 1999 Increased cortical bone mineral content but unchanged trabecular bone mineral density in female ERβ(−/−) mice. J Clin Invest 104:895–901
33. **Vidal O, Lindberg MK, Hollberg K, Baylink DJ, Andersson G, Lubahn DB, Mohan S, Gustafsson JA, Ohlsson C** 2000 Estrogen receptor specificity in the regulation of skeletal growth and maturation in male mice. Proc Natl Acad Sci USA 97:5474–5479
34. **Rossert J, Eberspaecher H, de Crombrugghe B** 1995 Separate cis-acting DNA elements of the mouse pro-α 1(I) collagen promoter direct expression of reporter genes to different type I collagen-producing cells in transgenic mice. J Cell Biol 129:1421–1432
35. **Yamazaki Y, Shimada T, Imai R, Hino R, Aono Y, Murakami J, Fukumoto S, Yamashita T** 2003 Elevated circulatory and expression level of fibroblast growth factor (FGF)-23 in hypophosphatemic mice. Bone 32:S88
36. **Beck L, Karaplis AC, Amizuka N, Hewson AS, Ozawa H, Tenenhouse HS** 1998 Targeted inactivation of Npt2 in mice leads to severe renal phosphate wasting, hypercalciuria, and skeletal abnormalities. Proc Natl Acad Sci USA 95:5372–5377
37. **Gupta A, Tenenhouse HS, Hoag HM, Wang D, Khadeer MA, Namba N, Feng X, Hruska KA** 2001 Identification of the type II Na(+)-Pi cotransporter (Npt2) in the osteoclast and the skeletal phenotype of Npt2−/− mice. Bone 29:467–476
38. **Panda DK, Miao D, Tremblay ML, Sirois J, Farookhi R, Hendy GN, Goltzman D** 2001 Targeted ablation of the 25-hydroxyvitamin D 1α-hydroxylase enzyme: evidence for skeletal, reproductive, and immune dysfunction. Proc Natl Acad Sci USA 98:7498–7503
39. **Donohue MM, Demay MB** 2002 Rickets in VDR null mice is secondary to decreased apoptosis of hypertrophic chondrocytes. Endocrinology 143:3691–3694
40. **Mansfield K, Rajpurohit R, Shapiro IM** 1999 Extracellular phosphate ions cause apoptosis of terminally differentiated epiphyseal chondrocytes. J Cell Physiol 179:276–286
41. **Amling M, Priemel M, Holzmann T, Chapin K, Rueger JM, Baron R, Demay MB** 1999 Rescue of the skeletal phenotype of vitamin D receptor-ablated mice in the setting of normal mineral ion homeostasis: formal histomorphometric and biomechanical analyses. Endocrinology 140:4982–4987
42. **Zhang MY, Wang X, Wang JT, Compagnone NA, Mellon SH, Olson JL, Tenenhouse HS, Miller WL, Portale AA** 2002 Dietary phosphorus transcriptionally regulates 25-hydroxyvitamin D-1α-hydroxylase gene expression in the proximal renal tubule. Endocrinology 143:587–595
43. **Azam N, Zhang MY, Wang X, Tenenhouse HS, Portale AA** 2003 Disordered regulation of renal 25-hydroxyvitamin D-1α-hydroxylase gene expression by phosphorus in X-linked hypophosphatemic (hyp) mice. Endocrinology 144: 3463–3468
44. **Flanagan JN, Wang L, Tangpricha V, Reichrath J, Chen TC, Holick MF** 2003 Regulation of the 25-hydroxyvitamin D-1α-hydroxylase gene and its splice variant. Recent Results Cancer Res 164:157–167
45. **Meyer Jr RA, Meyer MH, Morgan PL, Kiebzak GM, Roos BA** 1996 Effects of altered diet on serum levels of 1,25-dihydroxyvitamin D and parathyroid hormone in X-linked hypophosphatemic (Hyp and Gy). Bone 18:23–28
46. **Kiebzak GM, Roos BA, Meyer Jr RA** 1982 Secondary hyperparathyroidism in X-linked hypophosphatemic mice. Endocrinology 111:650–652
47. **Bai XY, Miao D, Li JR, Goltzman D, Karaplis AC** 2003 Early lethality in Hyp mice with targeted deletion of the Pth gene. J Bone Miner Res 18:S170
48. **Wang Q, Paloyan E, Parfitt AM** 1996 Phosphate administration increases both size and number of parathyroid cells in adult rats. Calcif Tissue Int 58:40–44
49. **Kremer R, Bolivar I, Goltzman D, Hendy GN** 1989 Influence of calcium and 1,25-dihydroxycholecalciferol on proliferation and proto-oncogene expression in primary cultures of bovine parathyroid cells. Endocrinology 125:935–941
50. **Fukagawa M, Okazaki R, Takano K, Kaname S, Ogata E, Kitaoka M, Harada S, Sekine N, Matsumoto T, Kurokawa K** 1990 Regression of parathyroid hyperplasia by calcitriol-pulse therapy in patients on long-term dialysis. N Engl J Med 323:421–422
51. **Gmaj P, Murer H** 1986 Cellular mechanisms of inorganic phosphate transport in kidney. Physiol Rev 66:36–70
52. **Murer H, Hernando N, Forster I, Biber J** 2000 Proximal tubular phosphate reabsorption: molecular mechanisms. Physiol Rev 80:1373–1409
53. **Zhao N, Tenenhouse HS** 2000 Npt2 gene disruption confers resistance to the inhibitory action of parathyroid hormone on renal sodium-phosphate cotransport. Endocrinology 141:2159–2165
54. **Soumounou Y, Gauthier C, Tenenhouse HS, Hoag HM, Martel J, Roy S** 2001 Murine and human type I Na-phosphate cotransporter genes: structure and promoter activity. Am J Physiol Renal Physiol 281:F1082–F1091

***Endocrinology* is published monthly by The Endocrine Society (http://www.endo-society.org), the foremost professional society serving the endocrine community.**